ZEPHYR, the Concept of a Compact Ignition Experiment

C. Andelfinger, M. Kaufmann, W. Köppendörfer, K. Lackner, and the ZEPHYR team *
Max-Planck-Institut für Plasmaphysik, EURATOM-Association, Garching

Z. Naturforsch. **37a**, 912–930 (1982); received June 11, 1982

To Professor Arnulf Schlüter on his 60th Birthday

The paper describes the physics background and the design of a compact ignition and burn control experiment (ZEPHYR). It was optimized with respect to magnetic field energy and costs on the basis of a cryogenically cooled normal conducting magnet. Ohmic heating, neutral injection and adiabatic compression were chosen to produce the required temperature. Ignition and controlled thermonuclear burn for about ten energy confinement times were foreseen.

1. Introduction

Heating of a tokamak plasma by α-particles will be a new heating method which in contrast to the conventional ones cannot simply be governed externally, but will depend in a highly non-linear way on the plasma state. For this reason, supporting studies in physically oriented devices are considered essential before its first application in a power producing reactor. Because of its nonlinear properties α-particle heating can realistically be studied only under conditions where it dominates the global energy balance, i. e. in an ignited or very nearly ignited state

From 1978 to 1980 IPP-Garching therefore defined and designed a compact ignition experiment, called ZEPHYR, with the following aims: to achieve ignition, to study α-particle confinement and to control the thermonuclear burn for several energy confinement times.

Besides calling for the development of material and components, successful operation of ZEPHYR required research and development in areas of decisive importance for fusion reactors; control of high power fluxes to the wall to minimize sputtering, concepts for stabilizing thermonuclear burn, design and development of components and equipment compatible with remote handling and safety provisions. These objectives were tackled within the frame work of an ignition experiment of minimum energy and heating power.

ZEPHYR was a conceptual design incorporating all essential technical components and technological developments. The study encompassed the assessment of the physical status, heating and burn control scenarios, the tokamak system with toroidal field magnet, the poloidal field system, the vacuum vessel and support structure, the peripheral systems, neutral injection, remote handling and repair facilities, the tritium system, diagnostics and nuclear safety [1].

This report presents the essential results of the ZEPHYR study and discusses the critical problems of physics and system components which governed the choice of parameters and dimensions. The results reflect what was regarded as technically feasible based on available technology. ZEPHYR was considered to be most effective solution with respect to its aims, underlying assumptions and constraints. Unfortunately, the project had to be sacrificed to budget restrictions.

Compact ignition experiments of the ZEPHYR type or as proposed by other groups [2, 3] are characterized by the small distance between plasma and magnet structure and the neglection of a blanket and nuclear shielding. The incorporation of a blanket and shield leads automatically to ignition systems of the INTOR (International Tokamak Reactor) or FED (Fusion Engineering Device) size and to a correspondingly costly system.

* ZEPHYR Design Team:

M. Blaumoser	H. Kollotzek	U. Schumacher
U. Broßmann	H. Kotzlowski	U. Seidel
R. Chodura	H. Krause	M. Söll
A. Elsner	H.-J. Kutsch	J. Sommer
H.-U. Fahrbach	F. Mast	B. Streibl
J.-H. Feist	E. Minardi	K. Tichmann
J. Gruber	J. Neuhauser	M. Ulrich
O. Gruber	M. Pillsticker	H. Vernickel
E. Harmeyer	H. Preis	H. Wegmann
W.-D. Hauben-berger	H. Röhr	H. Weichsel-gartner
W. Herrmann	W. Sandmann	R. Wilhelm
O. Jandl	H.-B. Schilling	R. Wunderlich
W. Kerner	W. Schneider	
	G. Schramm	

0340-4811 / 82 / 0800-0912 $ 01.30/0. — Please order a reprint rather than making your own copy.

In Sect. 2 the basic considerations which lead to the parameters are decribed. The regime is bounded by confinement constraints and the material stresses occurring in compact toroidal field (TF) magnets. The main additional constraints and the procedure for optimizing the tokamak system with respect to minimum magnetic energy and heating power are discussed as well. A summary of the dimensions and parameters thus derived for ZEPHYR is given in Section 3. The limited integral burn time due to irradiation damage of components and the inaccessibility of the tokamak system after a few DT discharges called for careful planning of the ZEPHYR discharge programme. Critical physical problems and their anticipated solutions as found by computational models are described in Section 4. Section 5 deals with the main components of the tokamak system. The shielding concept and problems of remote maintenance and repair are briefly treated in Section 6. The tritium handling concept is sketched in Section 7. Finally, the main conclusions drawn from the ZEPHYR study are summarized.

2. Basic Design Considerations

The definition of ZEPHYR proceeded as follows: firstly dimensions and parameters were derived from physics calculations and simplifying estimations of the technical constraints. Detailed calculations of thermal and mechanical stresses and compatibility tests of the components then lead to changes of the originally assumed data and in a second step of physical and technical calculations to the final parameter set. The following section presents this deduction in a concentrated way.

2.1. Determination of the Parameter Regime for Ignition

The physical requirements for ignition can be expressed in three conditions

- the fusion power produced in the form of energetic α-particles has to cover the energy losses of the plasma
- the major fraction ($\gtrsim 90\%$) of the energetic α-particles has to be confined in the system
- adequate power has to be provided to bring the plasma temperature into the thermonuclear regime.

Assuming an ideal deuterium-tritium mixture with $n_{\mathrm{D}} = n_{\mathrm{T}} = n_{\mathrm{e}}/2$ and $T_{\mathrm{e}} = T_{\mathrm{i}}$, the volume averaged energy balance condition can be written as

$$\frac{3\,\langle n_{\mathrm{e}}\,k\,T\rangle}{\tau_{\mathrm{E}}} = \left\langle \left(\frac{E_{\mathrm{DT}}}{20}\,\overline{\sigma v} - 4.8\times 10^{-37}\,\sqrt{T}\right) n_{\mathrm{e}}^2 \right\rangle \tag{1}$$

(in MKS units, T in keV). Here E_{DT} is the energy released per DT fusion reaction, $\overline{\sigma v}$ the velocity-space averaged fusion rate coefficient and τ_{E} a global energy confinement time. The second term on the right hand side describes hydrogen bremsstrahlung losses. Introducing the volume-averaged toroidal β by $\langle\beta_{\mathrm{t}}\rangle B_0^2/2\,\mu_0 = 2\langle n_{\mathrm{e}}\,k\,T\rangle$, this expression can be rewritten as

$$\langle\beta_{\mathrm{t}}\rangle\,\frac{B_0^2}{2\,\mu_0}\,\tau_{\mathrm{E}} = \frac{6\,\langle n_{\mathrm{e}}\,k\,\mathrm{T}\rangle^2}{\left\langle \left(\frac{E_{\mathrm{DT}}}{20}\,\overline{\sigma v} - 4.8\times 10^{-37}\,\sqrt{T}\right) n_{\mathrm{e}}^2 \right\rangle}\,. \tag{2}$$

The parameter combination $\langle\beta_{\mathrm{t}}\rangle B_0^2\,\tau_{\mathrm{E}}$ needed for self-sustained thermonuclear burn depends therefore on the average temperature and the form of the density and temperature profiles; the minimum assumed by it is approximately $2.4\,T^2\,s$ for homogeneous and $1.4\,T^2\,s$ for parabolic density and temperature profiles.

To apply (2) as a design criterium, assumptions about the achievable values of $\langle\beta_{\mathrm{t}}\rangle$ and τ_{E} have to be made.

In the circular ($\beta_{\mathrm{p}}\,A \ll 1$) limit, the global parameters determining ideal MHD stability

$$\beta_{\mathrm{p}} = 8\,\pi \int p\,\mathrm{d}f/(\mu_0\,I_{\mathrm{p}}^2),$$
$$q_{\mathrm{a}} = 2\,\pi\,a^2\,B_0/(\mu_0\,I_{\mathrm{p}}\,R),\quad A = R/a$$

in terms of the cross-sectional area integral of the pressure, the plasma current I_{p}, and the major and minor plasma radii are related by

$$\langle\beta_{\mathrm{t}}\rangle = \beta_{\mathrm{p}}\,\frac{1}{q_{\mathrm{a}}^2\,A^2} \tag{3}$$

A first approximation for β-limits used in the ZEPHYR design was obtained by inserting formally into this expression a low value for q_{a} routinely obtained in clean tokamak discharges ($q_{\mathrm{a}} = 2.35$), and $\beta_{\mathrm{p}} = A/2$, a limit beyond which equilibrium effects lead to large toroidal unsymmetries. These assumptions give

$$\langle\beta_{\mathrm{t}}\rangle_{\mathrm{limit}} = 0.09/A\,. \tag{4}$$

Subsequent detailed numerical exploration of stability limits with an ideal MHD stability code and a ballooning mode criterium [4] confirmed the scaling inherent in (4) as reasonable and approached the numerical value used for circular cross-sections to within 20%. In particular, however, experimental results becoming available during the ZEPHYR design phase [5, 6] and later [7] have justified this choice by exceeding our assumed limits by $\gtrsim 10\%$.

A considerable benefit in obtainable $\langle\beta_t\rangle$-values has been predicted by ideal MHD calculations for plasma columns with non-circular cross-sections [4]. Experimental evidence for this improvement, estimated to be of the form $\beta_t \sim (1+(b/a)^2)/2$ has, however, not been produced so far. As the basic version of ZEPHYR, for reasons described below, foresaw a major radius compression facility, incorporation of a non-circular plasma cross-section would have been very difficult and was not pursued further.

The parameter selection of the ZEPHYR experiment was based on the so-called ALCATOR-confinement scaling obtained from an analysis of a large sample of ohmically heated low Z_{eff}-discharges. In global design studies it was used in the form

$$\tau_E = 7.6\times 10^{-21}\,\langle n_e\rangle a^2\,[\mathrm{MKS}] \tag{5}$$

in one-dimensional transport calculations as

$$n_e\,\chi_e = 6.25\times 10^{19}\,\mathrm{m^{-1}\,s^{-1}}\,,$$
$$\chi_i = \text{neoclassical}\,,$$

where χ_e and χ_i stand for the electron and ion heat conductivities and $\langle n_e\rangle$ for the volume-averaged electron density. Similar assumptions were made later by the authors of the INTOR design study with slightly different numerical coefficients ($\tau_E = 5\times 10^{-21}\,\bar{n}\,a^2$, $n_e\,\chi_e = 5\times 10^{19}\,\mathrm{m^{-1}\,s^{-1}}$, $\chi_i = 3\times$ neoclassical); with $\bar{n}$ being the line average density).

The consequences of alternative confinement scalings are discussed in Section 4.2.

Substituting a confinement assumption of the above form into the energy balance equation yields

$$\langle\beta_t\rangle^2\,\frac{B_0^4\,a^2}{4\,\mu_0^2} = \frac{1.6\times 10^{21}\,\langle n_e\,k\,T\rangle^3}{\langle n_e\rangle\left\langle\left(\frac{E_{\mathrm{DT}}}{20}\,\overline{\sigma v} - 4.8\times 10^{-37}\,\sqrt{T}\right)n_e^2\right\rangle} \tag{6}$$

with the figure of merit $\langle\beta_t\rangle^2 B_0^4 a^2$ again depending on profile shapes and the temperature working point.

For parabolic profiles of n_e and T_e, the minimum requirement for $\langle\beta_t\rangle^2 B_0^4 a^2$ is $1.35\,\mathrm{T^4\,m^2}$; for practically more reasonable profiles with $n_e = \mathrm{const}$, $T = T_0(1-(r/a)^2)^2$ the value drops to 0.87, assumed for $T_0 = 12\,\mathrm{keV}$ [9].

The use of a pure heat conduction scaling of confinement times is justified only if significant radiative losses can be restricted to the outer layers of the discharge. This problem, together with other profile effects, is discussed below in Section 4.

A fraction of the α-particles born in thermonuclear reactions will be lost of the system before depositing their energy. For the design studied ripple associated losses in the compressed discharge state were small. The losses due to axisymmetric effects can be shown to depend on the product $I_p\,A$ only, with parameter combination $I_p\,A \geqq 7.5\,\mathrm{MA}$ resulting in 90% α-particle energy deposition in the plasma for assumed parabolic density and temperature profiles [10].

The scaling inherent in expression (6) strongly favours high-field, high current-density devices, suggesting thereby the use of purely ohmic heating for driving the plasma to ignition conditions. Because of the unfavourable temperature scaling of ohmic heating, the crucial question is whether by this method a high enough temperature can be reached for α-particle heating – with the opposite temperature characteristic – to take over. For a confinement law like (5) the temperature that can be achieved by ohmic heating alone scales like $(B_p/n_e\,\chi_e)^{0.8}$, with the poloidal field at the plasma boundary becoming thus the relevant figure of merit. One-dimensional transport calculations with the heat conduction coefficients given above yielded a value of $B_p = 3.5\,\mathrm{T}$ as required for ohmic heating to ignition, in good agreement – under the same assumptions – with calculations later reported in [11].

For the original technical lay-out of the device, the above conditions were used with an intermediate coefficient for the minimum required value of $\langle\beta_t\rangle^2 B_0^4 a^2 = 1.2\,\mathrm{T^4\,m^2}$. The ohmic heating requirements were first estimated with a simplified, more optimistic model as corresponding to $B_{p,\min} = 2.88\,\mathrm{T}$.

In this form the conditions:

energy balance: $B_0^4\,a^2\langle\beta_t\rangle^2 = 1.2\,F_t;\mathrm{T^4\,m^2}$, (7)

α-particle confinement: $B_0\,a/q_a \geqq 1.55$; Tm, (8)

Ohmic heating to ignition: $B_0 \geqq 2.88\,A\,q_a$; T, (9)

are used in Fig. 1 to define the regime of possible

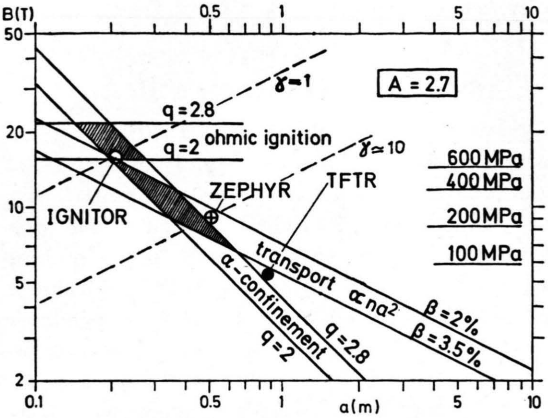

Fig. 1. Ignition regime in the B over a plane bounded by α-particle confinement and energy confinement conditions.

ignition experiments in the (B_0, a) plane for a fixed aspect ratio of $A = 2.7$.

F_t is a safety factor $\gtrsim 1$ which takes uncertainties in energy loss or α-particle heating efficiency into account.

Two lines are shown for each of the conditions (7) to (9), the lower representing the optimistic approach of $q_a = 2$ and $\langle\beta_t\rangle = 3.5\%$, the upper being based on the safer assumptions of $q_a = 2.8$ and $\langle\beta_t\rangle = 2\%$. The lower curves leave no safety margin for, e. g., less favourable energy confinement or impurity radiation losses. Below the horizontal lines of $B_0 = 15.6\,\mathrm{T}$ $(q_a = 2)$ or $B_0 = 21.8\,\mathrm{T}$ $(q_a = 2.8)$ ohmic heating is insufficient for reaching ignition and auxiliary heating is therefore necessary.

2.2. *Technical Constraints and Optimization*

Although ignition is attainable at least with auxiliary heating in the region above the transport and α-particle confinement line, technical constraints bound the area available in practice [12]. The mechanical stress limit of the TF magnet is soon reached for magnetic fields in excess of 10 T. Simplified, the average tensile stress in the TF magnet throat can be expressed by

$$\langle \sigma(\mathrm{MPa}) \rangle_{\mathrm{TF}} = 0.8\, B_0^2(\mathrm{T})\, g \tag{10}$$

with

$$g = \frac{\varkappa}{(A-\varkappa)\left[\left(1-\frac{\varkappa}{A}\right)^2 - \varrho^2\right]}.$$

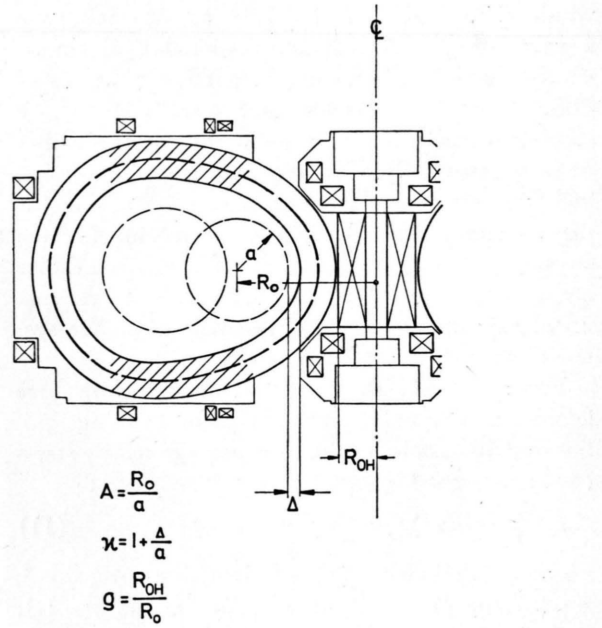

Fig. 2. Illustration of toroidal field coil contour and definition of the geometric quantities. The hachure indicates the area of lateral force support. The dash curve represents the bending moment free ideal contour.

This relation is obtained for bending-moment-free magnet contours with a curvature in the inner part of the magnet concentric with that of the meridional plasma cross-section. The factor g only contains relative geometric dimensions. It takes into account the fact that the area available for the TF magnet structure in the torus midplane is reduced by the space necessary for the vacuum vessel, limiter and wall armour structure, denoted by $\varkappa = 1 + \Delta/a$ and the space required for the ohmic heating (OH) transformer solenoid, normalized to R_0, denoted by ϱ. Figure 2 explains the normalized dimensions $\varkappa$ and ϱ.

An essential characteristic of compact ignition experiments is that the choice of $\varkappa \leqq 1.2$ excludes the possibility of shielding the magnet from nuclear radiation. The lifetimes of the magnet and tokamak system are consequently limited with respect to the integral thermonuclear burn time of the plasma. A discharge programme has therefore to assure that the aims of the experiment are likely to be reached within the available number of burn seconds.

In Fig. 1 tensile stresses obtained from formula (10) are indicated at the right for the particular B_0 values. Optimization and design studies of ZEPHYR which yielded $A = 2.7$, $\varkappa = 1.21$ and $\varrho = 0.3$ gave a value of $g = 3.78$. It is questionable of course whether g should be kept constant for tokamaks of different magnetic fields and size. Actually, g strongly varies with A, $\varkappa$ and ϱ, but determination of these, especially of $\varkappa$, requires a detailed design including stress analysis and material selection for the vacuum vessel. Keeping g constant, for the stress calculated in Fig. 1 was still a realistic choice because, for example, a reduction of the vacuum vessel structure more than proportional to the system dimensions is hardly possible.

For an IGNITOR type experiment, which here denotes a compact device capable of reaching ignition just by ohmic heating, the average tensile stress can be expressed by combining (9) and (10):

$$\langle \sigma(\mathrm{MPa}) \rangle = 6.63\, q^2 A^2 g\,. \tag{11}$$

Formula (11) yields $\langle \sigma \rangle_{\mathrm{TF}} \cong 700\,\mathrm{MPa}$ for $\varrho = 0.3$, $A = 2.7$, $q_{\mathrm{a}} = 2.4$ and a very optimistic $\varkappa = 1.1$. Reducing the aspect ratio to $A = 2.4$ and retaining the other values increases the stress to $\langle \sigma \rangle_{\mathrm{TF}} = 870\,\mathrm{MPa}$ on account of an increased g.

Of equal importance are thermal stresses. Compact tokamaks are limited in excitation time by the acceptable temperature rise of the normal conducting magnet. The integral of the square of the current density over the excitation time is limited for adiabatic heating:

$$\int_{t_0}^{t_1} j^2_{\mathrm{TF}}\mathrm{d}t \leqq \bar{\gamma}\, \frac{1}{f} \int_{T_0}^{T_1} \frac{c}{\varrho_\Omega}\, \mathrm{d}T\,; \tag{12}$$

j_{TF} is the current density in the magnetic throat, $\bar{\gamma}$ the average specific weight of the magnet, f the copper fraction of the total throat cross section area, c the heat capacity of the magnet and ϱ_Ω the specific resistance of the conductor. For cryogenically cooled magnets, organic insulation materials (epoxy resin) and a copper conductor

$$\int_{80\mathrm{K}}^{250\mathrm{K}} \frac{c}{\varrho_\Omega}\, \mathrm{d}t = 7 \times 10^{12}\, \frac{\mathrm{A^2\,sec}}{\mathrm{kg\,m}}$$

results as upper limit. Cryogenic cooling is required for maximizing the $\int (c/\varrho_\Omega)\,\mathrm{d}t$. 80 K corresponds to liquid nitrogen temperature prior to excitation and 250 K to the maximum allowed temperature after excitation. The latter temperature resulted from a detailed finite element stress analysis. The current density j can be written

$$j\left(\frac{\mathrm{MA}}{\mathrm{m}^2}\right) = \frac{1.6\, B_0(\mathrm{T})}{A\, a[(1-\varkappa/A)^2 - \varrho^2] f}\,. \tag{7}$$

The current density varies like $j \propto 1/a^2$ along the α-particle confinement path in Fig. 1 for a constant copper filling ratio f. For illustration JET has $j \cong 27\,\mathrm{MA/m^2}$, the ZEPHYR design value was $j = 144\,\mathrm{MA/m^2}$ and an IGNITOR type machine would need $j \geqq 300\,\mathrm{MA/m^2}$. The ZEPHYR value is larger than calculated from the $1/a^2$ dependance because half of the metal cross-section is covered by steel enforcement. This was because the material requirements for the ZEPHYR magnet were contradictory: high strength and large conductivity. An optimal solution for obtaining maximum values for (10) and (12) was to use austenitic steel cladded with copper. The desired properties of this compound were assured by a material development and test programme.

The attainable excitation time γ, measured in units of energy confinement time $\gamma = t_{\mathrm{pulse}}/\tau_{\mathrm{E}}$, characterizes whether the magnets are just suited to reach ignition or whether they can also be utilized to control and sustain the burn.

For the ALCATOR-INTOR confinement scaling and equal materials γ scales as $\sim A^2\, a/B^2$, disregarding possible limitations of the energy supply. ZEPHYR was designed to allow $\gamma \cong 10$ (Fig. 1), while IGNITOR type devices aim at $\gamma = 1$.

The extreme stresses and the small γ were the main causes for dispensing with the pure IGNITOR type concept and to choose an experiment instead located at the ZEPHYR position in Figure 1. For the heating power required then, additional to ohmic heating, neutral beam heating was planned, a method already sufficiently developed and proven at megawatt power levels. However, absorption in the plasma centre of the near-perpendicular injected power would have required a beam particle energy of

$$W \cong 1.8 \cdot 10^{-18}\, \bar{n}_{\mathrm{e}}\, a \cong 300\,\mathrm{keV}$$

owing to the large value of $\bar{n}_{\mathrm{e}}\, a \cong 1.6 \times 10^{20}\,\mathrm{m}^{-2}$ needed for ignition. Neutral beams of this energy had to be ruled out because of the poor neutralization efficiency of positive ion beams and because negative ion beam sources are not sufficiently developed. On the basis of a feasibility study conducted by LBL, Berkeley and IPP, 160 keV deuterium beams with a pulse length of 1.5 s were envisaged, an extension of the development work for the TFTR sources [13].

In order to match the line density requirements for ignition and neutral beam heating, plasma states with two different major radii were connected by adiabatic compression. Conservation of particles and magnetic flux [14] combine the heating requirements for the pre-compressed plasma and the ignition requirement for the post-compressed plasma to a major-radius compression ratio of $C \cong 1.5$ Detailed 1-d transport calculations yielded for the final ZEPHYR parameters an injection power of 16 MW, on the assumption that the injection power is divided among the three energy components 160 keV, 80 keV and 53.3 keV in the proportion 3 : 1 : 1. To account for impurity losses and additional loss effects, a power of 25 MW was finally envisaged.

Fitting two cycloids together for the ideal TF magnet contour at an aspect ratio of $A = 2.7$ for the compressed plasma allowed the toroidal magnet bore be effectively exploited (Figure 2). The advantages of this magnet form are discussed in Section 5.

The ohmic heating (OH) transformer coil in the central bore of the TF magnet entered the optimization procedure, particularly in determining ϱ and A [1]. The resistive and inductive flux consumptions required an OH flux of ± 5.5 Vs already reduced for the vertical field flux contribution. An OH coil design optimized with respect to the mechanical and thermal stress limits [15] allowed a central magnet bore as small as $R_{\mathrm{OH}} = 0.4$ m, finally yielding $\varrho = 0.3$ and $A = 2.7$.

The toroidal field magnetic energy was used as a measure of the effort and investment costs of the tokamak system, and the optimization procedure aimed to minimize the energy within the limits of the physical and technical constraints.

Expressing the TF magnetic energy by the ignition condition (1) and the mechanical stress relation (10) yields

$$W_{\mathrm{m}}(\mathrm{MJ}) \cong 9 \cdot 10^3 \varkappa^z \frac{F_{\mathrm{t}}}{\langle \sigma(\mathrm{MPa}) \rangle^2} \cdot \frac{C^{2.1}}{(\langle \beta_{\mathrm{t}} \rangle A)^3} \tag{13}$$

for $2.4 \leqq A \leqq 3.5$, where MHD stability limits $\langle \beta_{\mathrm{t}} \rangle A$ to 0.09. The aspect ratio of ZEPHYR was chosen within the permissible range of (13) after careful analysis of the influence of several, mostly technical, constraints. Because detailed analysis showed the exponent z to be about 5 for $1.1 \leqq \varkappa \leqq 1.25$, the magnetic energy strongly depends on the parameter $\varkappa$.

3. Summary of ZEPHYR Dimensions and Outline of an Experimental Programme

Table 1 gives the basic machine and reference plasma parameters.

Table. 1.

Basic Machine Parameters	Before compression	After compression
major radius R(m)	2.02	1.35
minor radius a(m)	0.61	0.5
aspect ratio A	3.3	2.7
compression ratio C	—	1.5
magnetic field on axis B_0(T)	6.1	9.1
flat-top time τ_{B}(s)		6.5
distance between plasma and coil Δ(m)		0.105
OH flux swing (Vs)	$\pm$ 5.5	
Reference Plasma Parameters		
I_{p}(MA)	2.3	3.7
$q_{\mathrm{rot}} = 1/t$	3.3	3.3
$q_{\mathrm{a}} = 2a^2 B_0/\mu_0 R I_{\mathrm{p}}$	2.4	2.3
$\langle\beta_{\mathrm{t}}\rangle_{\max}$ (%)	2	3.5
T (keV)	4.5...11.5	8...20
$\langle n_{\mathrm{e}}\rangle$(m^{-3})	1.1 — 2.2 $\times 10^{20}$	2.5 — 5 $\times 10^{20}$
τ_{E}(s)	0.3 — 0.5	0.5 — 0.8
integral burn time (s)		3000
Auxiliary Heating		
neutral beam power (MW)	25	
particle energy (keV)	160 (60% D^+)	
injection pulse time (s)	1.5	
injection angle to radius vector at $R = 2.02$ m	8° — 25°	

The following time szenario was envisaged for burning discharges: After an initial 200 ms ohmic heating phase in tritium with a plasma density approximately at the Murakhami limit, a neutral injection pulse of ≈ 1.1 s is to be applied followed by a compression of the plasma column to its final major radius within 100 ms. Thermonuclear burn should then set in, and thermal stability will be tested and controlled during the remaining 5.5 s.

The consequences of the compact layout of an ignition device on an experimental programme is now briefly outlined.

The spacing of 10 cm chosen between the plasma and toroidal field coils is occupied by the vacuum vessel structure and does not permit any shielding of the toroidal field coils against the neutron radiation from the plasma. Not only is a superconducting magnet therefore impossible but also the lifetime of a normal-conducting magnet is limited because of the degradation of the insulating materials by the neutron and secondary γ-radiation [16].

The shielding concept of ZEPHYR envisaged a first shield around the torus, termed the shielding house, of 0.7 m baryte concrete. The neutral injection boxes and pumping pipes are included there as well because of the large openings in the torus structure. The experimental hall outside the shielded tokamak system contains most of the diagnostics, which have to be accessible between discharges even when the torus structure is activated. The hall is designed as a second shielding of 2.5 m thick concrete walls for the remaining prompt neutron and γ-radiation and as a containment for activated air and leaking tritium.

The expected lifetime of the magnet insulation corresponds to a 10^{10} rad irradiation dose. A dose of 5×10^9 rad is equivalent to an ignited plasma of 3000 burn seconds. This constraint and the fatigue life time limitation required a carefully considered research programme which was divided into 10 000 full-load, 20 000 half-load and 40 000 quarter-load discharges, the latter for cleaning and wall conditioning. The experimental programme should consist of three phases.

The first phase should use hydrogen filling and injection and permit full access to the tokamak system. Owing to the reduced injection power the plasma parameters attainable should be considerably below ignition parameter values. In the second phase hydrogen filling should be used and deuterium injected. Plasma temperatures only 20% below the ignition value (10.5 keV) can be reached in this way. The neutron radiation will cause an activation level of 250 mrem/h in the torus structure after 1000 discharges, which will allow 100 man-hours of repair time per quarter-year if 10 persons are exposed to the permissible 2.5 rem per person. Repair time hands-on is therefore severely limited and special tools and automatic equipment are required. The third phase will finally use deuterium and tritium and produce 4×10^{19} neutrons/s in ignited discharges. After a few D/D discharges of 10.5 s duration the tokamak inside the shielding house is no longer accessible. Remote maintenance and repair of the vacuum vessel and magnet therefore had to be provided. According to the reference discharge programme 1000 D T discharges of short burn time and 500 discharges with 5 s burn time were foreseen.

4. Physics Considerations

Several uncertainties of the physics background used called for a critical discussion whether the margin provided by the layout of the experimental guaranteed sufficient safety for reaching the aims set. In addition, several effects and mechanisms had to be computed in greater detail, such as the toroidal field ripple influence on the particle and energy confinements or the energy transfer to the limiter and wall to minimize sputtering and impurity production. Development of acceptable schemes for burn control and shut down scenarios was required as well.

4.1. Performance Prediction for a Clean Plasma and the Standard Transport Model

Global confinement times depend both on heat conductivity and energy deposition profiles; in particular they contain also a weighted average of electron and ion confinement which depends on the division of the energy input among the two species and the degree of their collisional coupling. These effects – as well as impurity radiation losses – are conveniently taken into accout by one-dimensional transport calculations, which were accompanying each design decision and are reported in detail in [17–21].

These calculations were carried out using mainly the BALDUR transport code [22] including a Monte-Carlo description of the neutral particle dynamics, detailed neutral-beam deposition and slowing-down calculations, separate balance of the deuterium and tritium concentrations, first orbit losses of the fast α-particles and a time-resolved description of their slowing-down history, allowing to evaluate correctly the energy transfer to electrons and ions as well as the α-particle contribution to the total plasma pressure.

The effects of major radius compression were treated in a time-resolved manner and included also the increase in parallel and perpendicular energy of the slowing-down injection particles.

The parametric studies reported in [17], utilizing the "standard" transport model described before showed that under its assumptions and for an impurity-free plasma, ignition could be reached over a range of plasma densities by injecting a total neutron power of 16 to 17 MW into the plasma for one second, followed by adiabatic compression by a factor 1.5 in major radius. The characteristic time for compression (taken typically as 100 ms) was found to be an uncritical parameter, provided neutral injection was continued during this period. The $\langle \beta_t \rangle$-value required in these cases was 2.6%, including the contribution of the suprathermal, slowing-down α-particles.

4.2. *Effects of Alternative Scaling Assumptions*

Results of ohmic heating experiments becoming available during the later stages of the ZEPHYR design have demonstrated deviations from the simple Alcator scaling law (see (5)).

They were shown to be better fitted by an expression of the form [23]

$$\tau_{E,e} \sim \langle n_e \rangle \, a^2 \left[\frac{\langle T_e \rangle}{(I_p/R)^{2/3}} \right]^{\nu} \left(\frac{R}{I_p} \right)^{1/3} \left(\frac{a^2}{R^2} \right), \qquad (14)$$

where the exponent ν cannot be determined uniquely from ohmic heating experiments. Interpretation of experimental results in terms of local χ_e-values allows to narrow down the compatible T_e-dependences, suggesting $\chi_e \sim T^{-\gamma_1}$ with $0.5 < \gamma_1 < 1$ [24]. In particular, a good fit to a range of experiments (Pulsator, FT, Alcator-C, ASDEX) can be obtained using the so-called Coppi-Mazzucato law [25]

$$n \, \chi_e = c_1 \frac{B_0}{q(r)} \frac{a}{R} \frac{1}{T_e} \left(\frac{n_e}{A_i} \right)^{1/5} \qquad (15)$$

(with A_i the atomic weight), together with an enhanced Bohm-like transport within the $q = 1$ surface. For the data sets available for the study in [25], calculations with this confinement law allowed also to explain the roll-off in the $\tau_E(n_e)$ behaviour observed in the highest-density Alcator-C discharges [26].

Due to the favourable temperature dependence inferred by it, the use of (15) in computer simulations of non-ohmically heated ignition experiments leads to uniformly more favourable predictions than the original Alcator-scaling. For purely ohmically heated devices, this benefit is overcompensated by the implied unfavourable B_0 dependence-leading to a scaling of the maximum achievable temperature $\sim B_p^{2/3}$.

Early experimental results for discharges with strong neutral injection heating were found to be compatible with the Alcator-law [5] or even the Coppi-Mazzucato formula [27]. Since the termination of the ZEPHYR study, evidence for confinement degradation during neutral injection heating has been found in PDX [28], ISX [29] and ASDEX [30]. At present it is not clear whether this observed effect is due to a temperature or β-dependence of confinement or is a particularity accompanying strong neutral injection, and what conclusions are to be drawn from it for devices aiming at ignition or net power production.

4.3. *Toroidal Field Ripple Effects*

The ripple of the toroidal magnetic field caused by the discrete number of N toroidal field coils (tape-wound magnet concept) can lead to considerably enhanced energy and particle losses as a result of enhanced ion thermal transport, loss of ripple trapped and banana trapped injected ions, depletion of the high-energy tail of the thermal ions and, finally, loss of trapped fusion α-particles by ripple losses, the $N = 16$ coils producing a 6% ripple at the outer plasma edge. Calculations with the WHIST [31] code and the transport model described in [17] yielded intolerably high ripple losses for the combination of $N = 16$ coils, the chosen injection angle between 8 and 25 degrees (measured versus the radius vector) and the precompressed plasma position corresponding to $C = 1.5$. Several changes were discussed which combined would cure this problem: a decrease of the ripple amplitude and its radial decay length by increasing the number of coils to $N = 20$, a slight increase of the injection angle and an increase of the injection power by 1 to 2 MW.

The Bitter magnet concept was not affected by these considerations because of the sufficiently low ripple amplitude.

4.4. *Physics of Adiabatic Compression*

Basic problems associated with adiabatic compression arose from the necessity of rapid field variations, the need to keep the discharge well centered during its radial motion, and the complex balance of poloidal fluxes with the inherent danger of skin-current production for a high-conductivity plasma. The first two problems turn out to be closely linked, as the inhomogeneity of the induced fields contributes to the decay index $\tilde{n} = -\mathrm{d}\ln B_z / \mathrm{d}\ln R$, which has to remain within narrow bounds to yield both automatic vertical stability ($\tilde{n} > 0$) and a circular plasma cross-section at values of $\beta_p \geqq A/2$ ($\tilde{n} < 0.2$).

A computer code based on a Princeton diffusion code [32] was developed for calculating the eddy currents in the toroidal magnet coil structure, from which the vertical field variation and the decay index were determined in the plasma region. For a reliable check of the computed results measurements with a scaled model were made [33].

The avoidance of induced skin currents required a particular program for the OH circuit, which was determined by carrying out a sequence of flux conserving equilibrium calculations [34] for the case of adiabatic pressure variation. These calculations also yielded toroidal corrections to the usual adiabatic compression scaling formulas, and showed that, at least for the range of aspect and compression ratios considered, no strong interior profile distortion of pressures and current densities had to be expected.

Parametric studies, using the BALDUR transport code, were also conducted to assess quantitatively the benefit of the compression ratio [21]. Whereas large compression ratios give significant improvement in adiabatic heating and in the neutral injection deposition profiles, smaller compression ratios imply that the neutral injection takes place at larger values of $n\tau_E$ so that thermonuclear fusion will contribute more to the heating up. The achieved $\langle\beta_t\rangle$ after compression – a determining measure of the ignition probability – was found to increase monotonically with compression ratio. Runs with compression ratios $\gtrsim 1.2$ were found to ignite, indicating a certain reserve in the design. Smaller compression-ratio designs were also found to benefit from a lengthening of the injector pulse.

4.5. *Transport Calculations with Impurities and Wall Interaction Model*

Although high-density limiter-bounded tokamaks have been operated with low impurity concentrations in the plasma, the anticipated high power level of ignited ZEPHYR discharges would lead to an unacceptable impurity production by sputtering if the power flux to the wall were carried by particles. In principle, different schemes can be conceived in order to remedy this problem: reduction of the effective impurity confinement time, reduction of the plasma boundary temperature so that the single-particle energy falls below the sputtering threshold, and finally conversion of the heat flux and particle energy flow into impurity radiation in a suitable boundary layer. Calculational models [18, 35] were developed in order to investigate the possibilities of properly controlling the plasma boundary and the energy, particle and impurity fluxes. The 1 D tokamak transport code BALDUR was extended to include suitable boundary conditions. The studies were concentrated on iron impurities, this being a typical intermediate-Z material which has the desirable characteristics of radiating predominantly in the boundary zone with a temperature below 1 keV.

For sufficiently central heating, e. g. α-particle heating or an idealized model for ICRH, stationary equilibria with effective radiation cooling at the boundary were found for a wide range of model assumptions. Because of self-limitation of the production rate, the impurity content in the plasma bulk for these models remained tolerable although the residual sputtering rate at the walls and the corresponding erosion strongly depended on the assumed efficiency of the impurity pumping by the limiter and the impurity transport in the plasma.

Figure 3 shows as an example a solution with a fully developed, stable radiation layer for the burn phase of a ZEPHYR discharge. The range of model

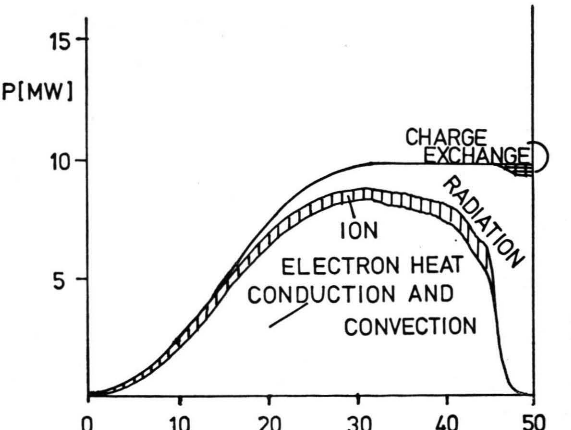

Fig. 3. The formation of a cold plasma mantle as seen from the loss powers integrated over the volume with radius r, from calculations assuming anomalous impurity transport and neoclassical accumulation.

assumptions compatible with such physically desirable solutions was found to be considerably narrowed for weakly penetrating neutral beam heating.

The throat section of the vacuum vessel would have to take the largest power flux density and was therefore designed with a covering of graphite knobs as wall armour. For a homogeneous power flux distribution – if all power is radiated from the plasma – 0.7 MW/m^2 are obtained. This value increases to 3 MW/m^2 if half the power is transported by thermal conduction and half by radiation. More details on the limiter design are given below.

4.6. Burn Control

Several promising methods for stabilizing the thermonuclear burn have been extensively studied by the Massachusetts Institute of Technology (MIT) and the MPI für Plasmaphysik (IPP) [36]. The methods suitable for testing in ZEPHYR were based on major-radius variation, ripple effects and feedback-controlled additional heating at high Q values (Q = fusion energy output/average additional heating power).

On the assumption of particle and magnetic flux conservation and for a confinement scaling law

$$\langle n_e \rangle \tau_E = 7.6 \times 10^{-21} \langle n \rangle^2 a^2 ,$$

an ignition curve can be calculated in the average temperature $\langle T \rangle$ versus major radius R_0 plane, with ignition being defined by the balance of energy

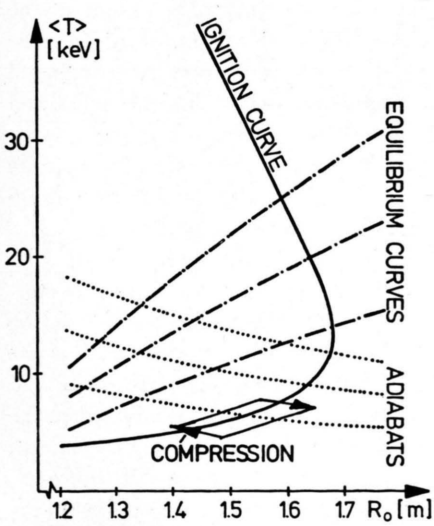

Fig. 4. Principles of burn control of the ignited plasma by major radius (R_0) variation.

losses and α-particle heating (Figure 4). In the same plasma "equilibrium" curves can be defined which describe the path of the tokamak discharge in the R, $\langle T \rangle$ plane due to temperature changes in a given time-constant vertical field. Stability of equilibrium depends on the type of intersection of the two curves, which can be controlled by feedback controlling the vertical field value. As a third family of curves "adiabats" describe the variation of the plasma state for sufficiently fast externally enforced position changes.

On the basis of these curves, cycles in the R, $\langle T \rangle$ plane can be defined by which energy can be put into the plasma or extracted from it. In order to utilize these curves for stabilization, the initially overignited plasma is, for example, moved by a finite amount into the underignited region, where it is left to cool down over a certain period, to be brought back later into the ignited region, again approximately along an adiabat. By appropriately choosing the amount of radial displacement and duration of the cooling period one has a large amount of external control of the burn.

This burn stabilization method based on plasma displacement and its application to ZEPHYR is described in detail in [36].

The effects of main-field ripple on confinement can be applied to burn stabilization in two basic ways. In time-independent ripple, the strong temperature dependence predicted for the associated ion heat conduction losses should tend to stabilize thermal runaway at comparatively low burn temperatures. Time-dependent ripple, for which the ripple amplitude is increased in response to an observed enhancement in fusion output, could in addition act by increasing the fractional loss of fast α-particles, thereby reducing the plasma heating rate. In ZEPHYR adjustable ripple can be obtained by superposing on the toroidal coil current a component with alternating sign in adjacent coils or modules: the required arrangement of the current feeds to the main field coils agrees with that chosen anyway for minimizing the consequences of possible coil failure. As this current component, to lowest order, does not change the energy content of the main field, fast enough ripple changes should be possible in ZEPHYR to utilize them also in feedback fashion.

Burn stabilization by feedback-controlled additional heating has been studied both by stability analysis without reference to specific machine parameters [36] and by one-dimensional, time-dependent simulation calculations for ZEPHYR parameters using the WHIST code [20].

It has also been suggested to operate a fusion reactor in a thermally stable, higher temperature regime [37]. A basic drawback of this so-called hot-ion mode is the increased contribution of the super-thermal α-particles to the total plasma pressure because of the increase in their slowing-down relative to the total energy confinement time. Operation of ZEPHYR was, however, also foreseen in this regime.

5. The Tokamak System

The tokamak system design (Fig. 5) consisted of the toroidal field (TF) magnet, the poloidal field (PF) system, the vacuum vessel, the magnet cooling system and the energy supply. In the following, only features of special interest of these components are described. One basic design principle of the tokamak system was to provide remote exchange and repair of components. The TF magnet and the vacuum vessel were therefore devided into octants whose separation planes allowed removal and insertion of whole octant units. Robots were designed for the necessary cutting, welding and bolt connections. Outside the experimental hall shielded rooms were designed for remote repair of defective parts.

5.1. The TF Magnet

Two competitive TF magnet concepts were investigated both using cryogenically cooled, steel-reinforced copper conductors. The tape-wound TF magnet [38] consisted of 16 strongly tapered pancake coils based on a C/D constant tension shape with C-section suspended freely in the force field in order to allow thermal expansion of the tapered section. The centering and overturning forces were balanced by rigid casings around the outer part of the coils and by structural wedges between the coils. By means of analytic and finite element calculations the design was optimized with respect to magnetic force support and thermal expansion. The design of the magnet made use of a study of BBC, a producer with the relevant experience.

MIT [39] and IPP Garching [40] worked out Bitter-type TF magnets one of which balanced the overturning forces by frictional shearing stresses, whereas the other put a casing around sectors of Bitter plates and used form locking for force balance. The Bitter plates consisted of copper-steel plates which had to be combined at least in the critical inner section of the magnet. The mechanism of the Bitter magnet relied essentially on the control of a proper lateral pressure distribution, which proved to be difficult because of thermal expansion. The tape wound magnet was at an advantage in this respect because the pancake coils were laterally free and rigid in the throat.

Finally, a control of tensile and pressure stresses of 350 MPa and 200 MPa due to the toroidal field force appeared possible for both magnet concepts. Considerable effort, however, was necessary to distribute the shearing stresses properly, e. g. by means of epoxy resin filled cushions, which had to be limited to a maximum of 30 MPa because of the insulation. A sliding friction zone was necessary in certain positions, e. g. where the tape-wound coils leave the magnet casings in order to stay below the shearing stress limits.

The magnet designs were accompanied by material dvelopment and test programmes, the largest being that for the steel-plated copper conductor. Warm pressing and explosive plating of copper on steel and successive cold rolling proved successful [41] at least for strips of the size necessary for the tape-wound magnet. Figure 6 gives test results in the form of survival probability of a sample at the required stress level. The development of full-size (2.5×3 m) Bitter plates could not be concluded although some promising results had already been obtained [42].

Difficult for the Bitter magnet was to incorporate the port openings for neutral injection and diagnostics and to work the plates around them.

The tape-wound magnet was designed for LN_2 cooling by pipes at the edge of every 7th conductor. The calculated and experimentally tested cooling time between excitation pulses was 50 min. For the Bitter magnet LN_2 bath cooling was envisaged.

When the ZEPHYR project was terminated at the end of 1980, the final choice of the magnet concept had not been made. The IPP group felt, however, that the tape-wound magnet concept was better developed, its functioning more transparent and the conductor production secured.

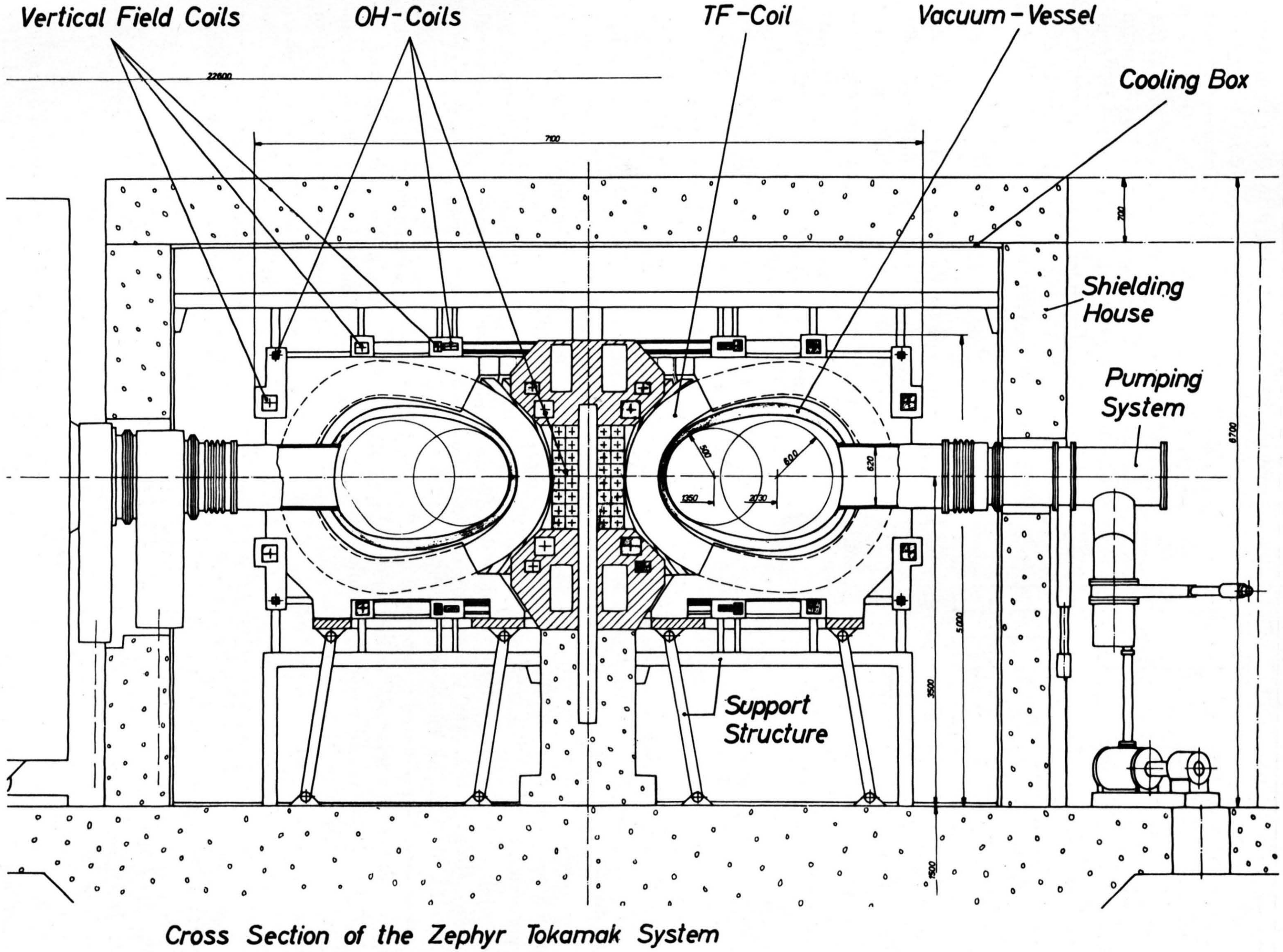

Fig. 5. The ZEPHYR tokamak system.

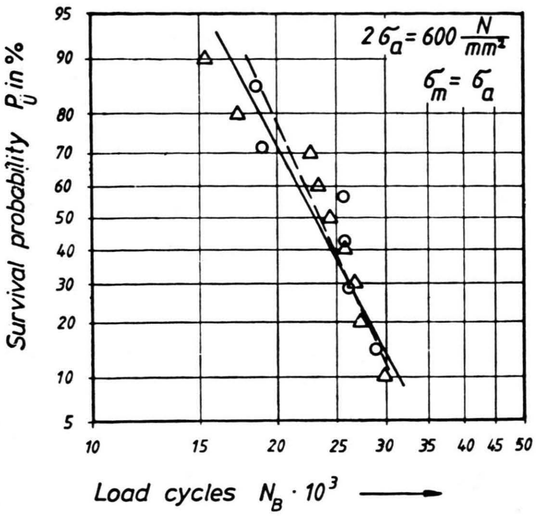

Fig. 6. Survival probability of the steel copper compound. △——△ Blast plated and cold worked; ○---○ plated with intermediate layer and cold worked.

5.2. *The Central Transformer Coil*

The poloidal field coils [43] were divided into ohmic heating and vertical field coils for equilibrium control and compression. The technically critical coil was the central transformer, which had to be optimized with respect to mechanical and thermal stresses. The required symmetric flux swing of 11 Vs through an aperture of 0.38 m radius produced a maximum of 28 T. The 0.28 m thick coil had to be optimized with respect to radial and circumferential stresses. This was achieved by dividing the coil with two slits into three concentric cylinders, thus removing the radial tension force exerted by the outer cylinders on the inner ones. This reduced the maximum stress (circumferential) to 400 MPa. The slits were filled with mica. Each coil cylinder consisted of two winding layers of a copper alloy conductor (Cu, Cr 1%, Zr 0.15%) with a cross-section $42 \times 32\,mm^2$ and cooling channel with diameters varying from 7.9 to 15.5 mm, depending on the winding length, in order to obtain equal temperature difference between all inlets and outlets. To keep the thermal stresses within acceptable limits, the coil had to be cooled down to 30 K by gaseous helium prior to excitation.

This central transformer coil was calculated and designed in close cooperation with industrial firms, who were awarded study contracts in order to ascertain production capability at the outset.

The other poloidal field coils posed no special problems. They were arranged to allow remote replacement. In order to perform adiabatic compression, the magnetic energy in the equilibrium coil system had to rise by 50 MJ within 100 ms. This was accomplished by inductive storage of 144 MJ and a nominal disrupting power of 1.6 GVA with an ohmic transfer element. Breakers of the JET type were envisaged. The total energy and power consumptions in the OH and VF systems amounted to 800 MJ and 360 MW, respectively.

5.3. *Vacuum Vessel and Limiter*

The small space in the throat ($\Delta = 0.1$ m), the electric resistance requirements and the loads on the vessel governed the design of the vacuum vessel. The most severe load was calculated from the three lowest eigenmodes of decaying eddy currents caused by hard plasma disruptions [44]. The all-metal vessel consisted of 16 wedge-shaped double-wall shell sectors connected toroidally with steel bellows. The bellows provided the required toroidal resistance ($\approx 1\,m\Omega$), while the shell sectors provided stiffness and, through its ports, access for assembly, testing, pumping, neutral injection and diagnostics. Originally, INCONEL was envisaged as material but later replaced by a more conventional stainless steel because of reduced activation due to the smaller nickel content.

The throat part and all bellows were protected by a large limiter structure consisting of individual graphite knobs of about 40 mm in diameter (Figure 7). The plasma was bounded in this way by 16 poloidal limiters prior to compression, and by the total throat area limiter in the compressed state. A TiC coating on the limiter knobs was foreseen to reduce methane formation. The limiter knobs were designed to allow remote replacement by a robot.

The development and test programme for the limiter knobs and the attainable energy flow to the backing plate was continued after the ZEPHYR project was terminated [45].

6. Peripheral Systems

6.1. *The Building Concept*

The main object of the building design was safety of the general public and operating personnel. The centre of the building was the experimental hall with

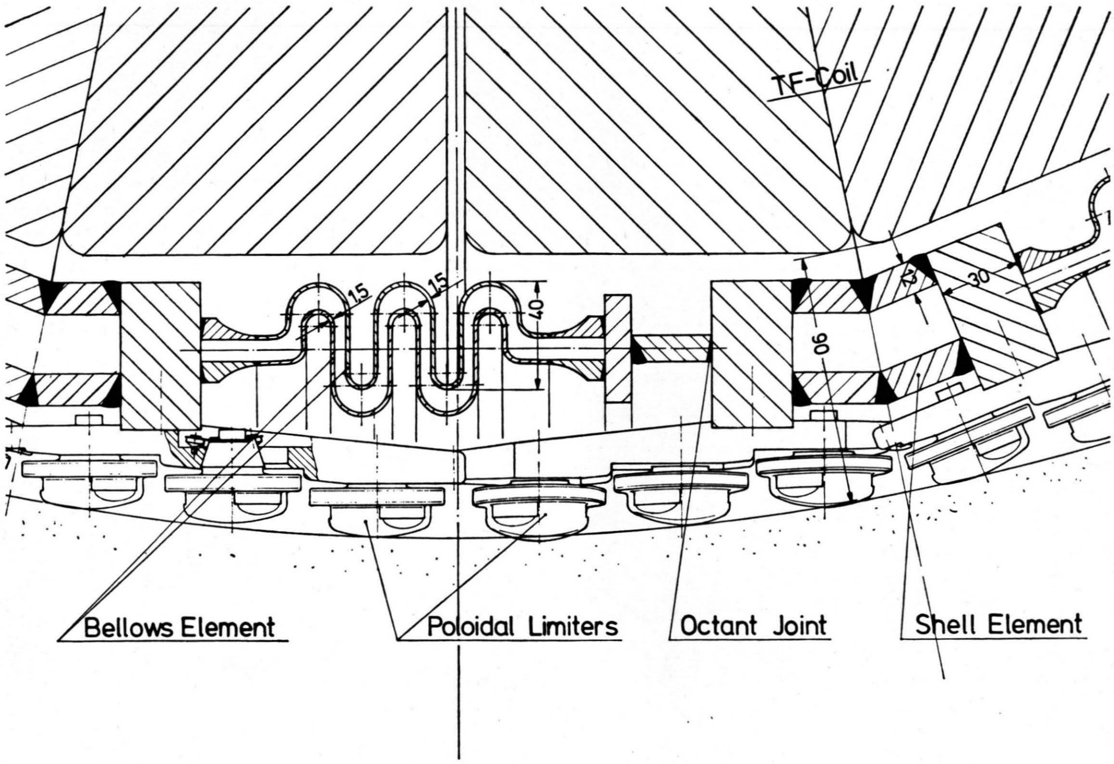

Fig. 7. Structure of the vacuum vessel and limiters.

the shielding house. A 1 D model [46] was used for calculating prompt and delayed neutron radiation and activation of the structure. Recently, the effect of openings in the shielding house was calculated by means of a 2 D computer model in cooperation with an institute at Stuttgart University [47].

The tokamak system and the neutral injection boxes were enclosed by the shielding house. Diagnostic equipment was located outside the shielding house in the experimental hall. The walls of the experimental hall together with the shielding house guaranteed sufficient protection against the dominant prompt neutron and γ-radiation. Hot cells for repair of activated components and a hot storage room were put adjacent to the experimental hall and connected by sluices (Figure 8). The basement of the experimental hall contained room for diagnostic apparatus and neutral injection auxiliary equipment, the tritium handling room, the tritium absorption system and a storage room for tritium-contaminated materials.

Three areas were distinguished:

Area I: All rooms outside the experimental hall, their basements and hot cell. Unlimited access possible.

Area II: Basement of experimental hall. No access during D-T discharges. Limited access at other times. Connections by tubes and channels to the inside of the shielding house. Release of tritium possible. Strong ventilation system connected with tritium absorption system provided. Possible activities: Ar^{41}: 10^{-7} Ci/m^3, N^{13}: 10^{-6} Ci/m^3, N^{16}: 2×10^{-4} Ci/m^3 and tritium: 2×10^{-5} Ci/m^3. – Protective clothing with oxygen apparatus possibly necessary.

Area III: Experimental hall outside the shielding house and basement for water cooling of the neutral beams lines. Access limited by activated air, tritium contamination and radiation from activated materials. Expected activation of air per discharge: Ar^{41}: 2×10^{-6} Ci/m^2, N^{13}: 2×10^{-5} Ci/m^3, N^{16}: 5×10^{-3} Ci/m^3 and T: 2×10^{-5} Ci/m^3. – The ven-

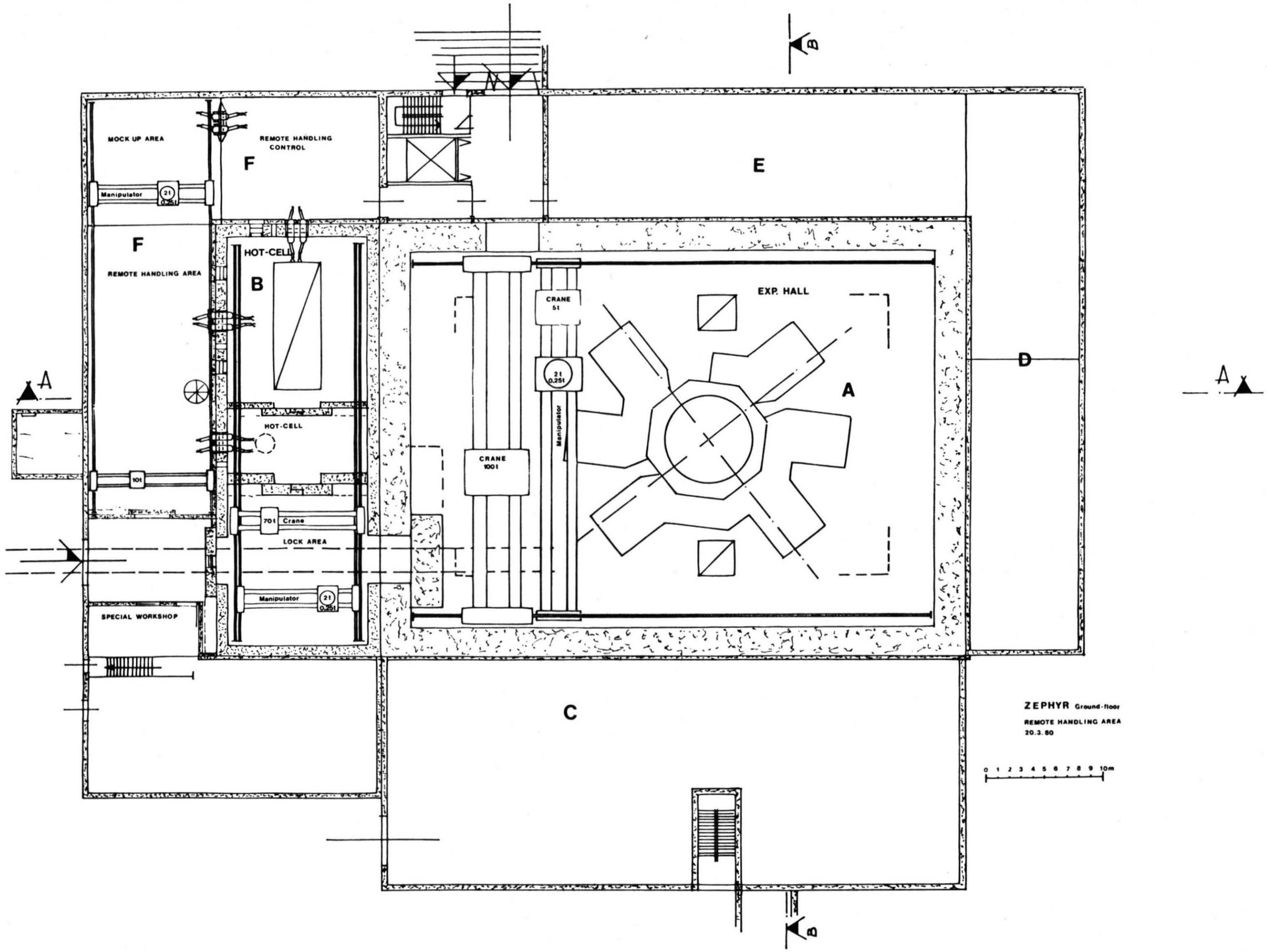

Fig. 8. Design of the experiment and building (top view).

tilation system should allow access after $1-2$ hours with protective clothing and oxygen apparatus. The γ-radiation of activated structure in the case of D-T discharges after radiation equilibrium has been achieved will cause 50 mrem/h after 5 h, 23 mrem/h after 15 h and 0.32 mrem/h after 10 d waiting time. Repair personnel can therefore only be exposed several tens of hours to the experimental hall. Maintenance and manipulation of components in the experimental hall should therefore be carried out remotely as much as possible by manipulators and robots. Working times hands-on should be saved for difficult handling. Diagnostic devices should therefore also be equipped with elements for remote control and adjustment.

Area IV: Interior of shielding house. No access for hands-on work, full remote handling required. Replacement of defective components by automats and manipulators, transportation by remotely controlled cranes to the hot cell. Repair should be carried out as much as possible in the hot cell with direct observation by manipulators.

6.2. The Tritium System [48]

The 3000 burn seconds of ZEPHYR would require 10^6 Ci of tritium in total.

By processing and recycling tritium at the experiment, however, a considerably smaller amount of tritium, $<10^5$ Ci, would have sufficed.

The – strongly simplified – proposal for the tritium cycle was as follows: the tritium is stored in uranium beds as UT_3. Controlled heating releases the required amount to the tritium injection system. There it is mixed with deuterium to supply the torus. The exhaust from the torus vacuum system is collected in storage tanks and purified of water and hydrocarbons. The hydrogen isotopes are then separated in the tritium separation system. A small-scale gaschromatographic separation unit was developed for this purpose and is being enlarged at present for larger throughput values because of its general importance for other ignition devices beyond ZEPHYR [49]. This choice was governed by the lower tritium inventory of this method as compared with cryogenic distillation.

All larger tritium inventories, such as the tritium storage tank, the purification system, the isotope separation, the forevacuum system and the storage, were located in the tritium-handling rooms in secondary containments, mostly glove boxes. Three tritium absorption systems had to remove tritium from the torus exhaust, from the inert gas atmosphere of the secondary containments and from the air in the tritium-handling room and the experimental hall, the latter being the most powerful one, with a throughput of 3000 m^3/h. Finally, the German radiological regulations had to be met: 4.8×10^{-6} Ci/m^3 for control area, 4.8×10^{-7} Ci/m^3 for the supervised area and 10^{-8} Ci/m^3 for the public area.

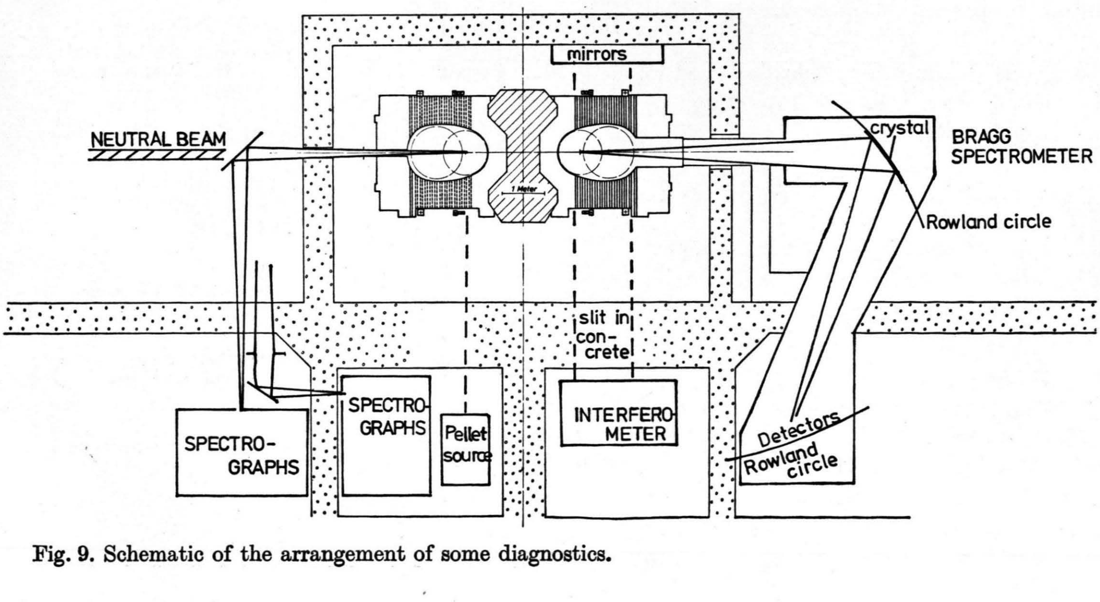

Fig. 9. Schematic of the arrangement of some diagnostics.

6.3. *Remarks on Diagnostics for ZEPHYR*

Diagnostic methods now used or under development for tokamaks had to be envisaged for ZEPHYR in order to utilize efficiently the limited experimental time of 10 000 full-load discharges.

Three problem areas required careful planning of the diagnostics. The first was the limitation on the number and size of diagnostic port holes. The second was the remote handling of diagnostic apparatus because of the prompt and delayed neutron and γ-radiation. The third was the radiation on the detectors.

The favourite place for diagnostics was the basement under the shielding house. The 1.5 m concrete ceiling reduced the radiation level sufficiently to allow access after a waiting-time of a few hours even after 3 years of D-T operation. Typical diagnostic arrangements are shown in Figure 9.

All equipment in the experimental hall used for D-T plasma diagnostics had to be designed for remote control and adjustment because the limited access for manual work could not be used for; e. g., aligning diagnostics. Windows and lenses in the direct radiation field should not suffer from permanent or transient absorption effects. Luminescence caused by the radiation field was estimated to be negligible compared with the bremsstrahlung background from the plasma.

Inside the shielding house no detector could be allowed except magnetic probes. For insulation inorganic material or possibly kapton was preferred in this area.

All shielding house diagnostic penetrations had to be sealed by windows or foils for providing the second tritium containment.

7. Summary and Conclusions

The ZEPHYR project was a D-T burning compact tokamak design clearly complementary to JET with the aim of ignition and burn control. On the basis of the ALCATOR-INTOR energy confinement scaling it guaranteed ignition with a safety margin of a factor 1.5 in energy confinement time. For ignition it required about one-third of the auxiliary heating power (over 1.5 seconds) which JET requires at present for ignition in its second phase.

The tokamak system design of ZEPHYR was considered to be the most economic approach to ignition and burn control. Using neutral injection with particle energies of 160 keV as an essentially proven auxiliary heating source in conjunction with adiabatic compression, optimization and design lead to a compact high-field high-density tokamak with a cryogenically cooled normal-conducting magnet. The limited lifetime of the magnet due to degradation of insulator material by nuclear radiation allowed at least 3000 burn seconds of operation in the ignited state. An experimental programme consisting of hydrogen discharges and hydrogen deuterium discharges prior to the deuterium tritium discharges guaranteed the optimal use of 10 000 full-load discharges and numerous discharges at reduced magnet load.

The critical components according to the optimization were the toroidal field magnet, the central transformer coil and the vacuum vessel. All three had to be designed up to the stress limits of available materials as a consequence of stringent space requirements. Two magnet concepts were pursued: the tape-wound magnet and the Bitter magnet, both relying on the strength of a copper-clad steel compound conductor. A material development and test programme was carried out which afforded a good outlook for the production of the compound con-

Table 2.

Collaborating Institutes	*Industrial Contributions*
KFK, Karlsruhe Safety matters Tritium Propagation Remote Handling, etc.	Vacuum Technology, Tritium; Balzers, Leybold-Heraeus, Nukem, Pfeiffer
IKE, Stuttgart Shielding Calculations	Coil Materials: Dynamit Nobel, IABG, Kabelmetall, Krupp, Vakuumschmelze Hanau, VDM, etc.
GSF, Neuherberg Irradiation of insulators	
TUM, Institut für Radiochemie Tritium permeation	TF Coil: BBC, MBB, Siemens-KWU
LBL, Berkeley	
ORNL, Oak Ridge Neutral Injection	Remote Handling: Messer-Griesheim, Wälischmiller
MIT, Cambridge Magnet Technology	
LASL, Los Alamos	Shielding, Nuclear Ventilation: Lahmeyer, KWU
PPPL, Princeton	Cooling: Linde, Sulzer
Sandia, Livermore	

ductor as well as for the thermally highly loaded limiter.

No material or magnet design solution was found which might possibly meet up to the requirements of an IGNITOR type experiment, an ohmically heated ignition tokamak.

Although ZEPHYR aimed at the lowest possible investment costs by optimizing the tokamak system and heating power, the project was, however, – as it can be expected for all DT-experiments reaching ignition – considerably burdened by the estimated investment costs for the peripheral systems required for remote handling and repair, radiation protection, tritium handling and safety.

Acknowledgement

The authors are grateful to Prof. A. Schlüter and Prof. R. Wienecke for continuous support and stimulating discussions. The ZEPHYR project team gained major support, arranged through the US Department of Energy (DOE), from the Lawrence Berkeley and Livermore Laboratories, Massachusetts Institute of Technology (MIT, Cambridge) and Princeton Plasma Physics Laboratory in the fields of neutral injection, magnet design and general tokamak technology. A complete list of research institutes and industrial companies which were involved in the ZEPHYR development programme is given in Table 2.

[1] Investigation for the ZEPHYR Ignition and Burn Experiment, C. Andelfinger, M. Kaufmann, W. Köppendörfer, K. Lackner, J. Neuhauser, and H.-G. Wegmann, IPP Garching ZEPHYR-Report No. 32, Juli 1980.
[2] D. R. Cohn, R. R. Parker, and D. L. Jassby, Nucl. Fusion **16**, 31 (1976); D. L. Jassby, D. R. Cohn, and R. R. Parker, Nucl. Fusion **16**, 1045 (1976).
[3] B. Coppi, Comments Plasma Physics Contr. Fusion, 1977, Vol. 3, No. 2, pp. 47–62, B. Coppi, L. DeMenna, F. Esposito, and F. Laudiore, Proc. Course Varenna, Italy, Sept. 1977, p. 247, Pergamon Press, London 1977.
[4] W. Kerner, P. Gautier, K. Lackner, W. Schneider, R. Gruber, and F. Troyon, Nucl. Fusion **21**, 1383 (1981).
[5] M. Murakami et al., Proc. 8th Int. Conf. on Plasma Physics and Contr. Nucl. Fusion Research, IAEA, Vienna 1981, Vol. I, p. 377.
[6] N. Suzuki et al., Proc. 8th Int. Conf. on Plasma Physics and Contr. Nucl. Fusion Research, IAEA, Vienna 1981, Vol. II, p. 525.
[7] R. J. Fonck et al., 5th Int. Conf. on Plasma Surface Interactions in Controlled Fusion Devices, Gatlinburg (USA), May 1982.
[8] International Tokamak Reactor, Zero Phase, IAEA, Vienna 1980, p. 85.
[9] K. Lackner et al., Proc. 2nd Joint Grenoble Varenna Int. Symp. Como, Sept. 1980, Vol. 2, 1076.
[10] D. G. McAlees, ORNL-Report, TM-466 (1974), Calculation of Alpha Particle Heating in Tokamaks, D. Mikkelsen and D. Post, unpublished (1978).
[11] C. O. Wagner, Phys. Rev. Lett. **26**, 654 (1981).
[12] W. Köppendörfer, Proc. 11th SOFT, Oxford 1980, p. 77.
[13] J. H. Feist, W. Herrmann, and E. Speth, Proc. 11th SOFT, Oxford 1980, p. 975.
[14] H. P. Furth and S. Yoshikava, Phys. Fluids **13**, 2593 (1970).
[15] ZEPHYR-Poloidal Field System, U. Seidel, IPP Garching Report 1/201, April 1982.
[16] Toroidal Field Magnets for ZEPHYR, Tape and Bitter Concepts, Conductor and Insulation Materials, E. Breit, U. Broßmann, J. E. Gruber, W. D. Haubenberger, O. Jandl, S. Kamm, F. Mast, S. Mukherjee, M. Söll, E. Springmann, and B. Streibl, IPP Garching Report 1/192 (1981).
[17] Transport Calculations with the BALDUR Code, K. Lackner and R. Wunderlich, IPP Garching Report 1/178, December 1979.
[18] Self-Limitation of Impurity Production by Radiation Cooling at the Edge of a Fusion Plasma, J. Neuhauser, K. Lackner, and R. Wunderlich, IPP Garching Report 1/198, April 1982.
[19] O. Gruber, K. Lackner, J. Neuhauser, W. Schneider, and R. Wunderlich, Proc. 2nd Joint Grenoble Varenna Int. Symp. Como, Sept. 1980, Vol. 2, 1075.
[20] 1D Calculations on Transport Neutral Injection Heating and Ignition Control in ZEPHYR, O. Gruber, IPP Garching Report 1/1977, December 1979.
[21] Computations on Neutral Beam Injection Heating, Ripple Recommendations and Varying Compression Ratio in ZEPHYR, O. Gruber, K. Lackner, G. Lister, IPP Garching Report 1/199, April 1982.
[22] D. E. Post, C. E. Singer, and A. McKenney, TFTR Physics Group Report 33, PPPL, January 1981.
[23] U. Ascoli-Bartoli et al., 9th Europ. Conf. Contr. Fusion and Plasma Physics, Oxford 1979, p. 261.
[24] O. Gruber, Bull. Amer. Phys. Soc. **26**, 943 (1981).
[25] B. Coppi and E. Mazzucato, Phys. Letters **71 A**, 337 (1979).
[26] S. Fairfax et al., Proc. 8th Int. Conf. on Plasma Physics and Contr. Nucl. Fusion Research, IAEA, Vienna 1981, Vol. 1, p. 439.
[27] W. Stodiek et al., Proc. 8th Int. Conf. on Plasma Physics and Contr. Nucl. Fusion Research, IAEA, Vienna 1981, Vol. 1, p. 9.
[28] H. P. Eubank et al., 3rd Joint Varenna-Grenoble Int. Symp., Grenoble, March 1982, paper A2.
[29] P. H. Edmonds et al., ibid, paper A1.
[30] E. Speth et al., ibid, paper A4.
[31] W. A. Houlberg and R. W. Conn, Nucl. Sci. Eng. **64**, 141 (1977).
[32] H. Preis, Arch. Elektrotechn. 1982, in press.
[33] Diffusion of the Vertical Field into the Tape-Wound Magnet, N. Gottardi, F. Mast, H. Preis, and R. Süß, IPP Garching Report 1/189, July 1981.
[34] D. B. Albert, Nucl. Fusion **20**, No. 8, 939 (1980).
[35] K. Lackner and J. Neuhauser, Proc. IAEA Meeting on Divertors and Impurity Control, Garching 1981, p. 58.

[36] K. Borrass et al., Proc. 8th Int. Conf. on Plasma Physics and Contr. Nucl. Fusion Research, IAEA, Vienna 1981, Vol. 1, p. 619 (1980).
[37] J. F. Clark, Nucl. Fusion **20**, 563 (1980).
[38] H. Broßmann, J. E. Gruber, W. D. Haubenberger, O. Jandl, M. Söll, and B. Streibl, Proc. 11th SOFT, Oxford 1980, p. 467.
[39] H. Becker and J. E. C. Williams, Proc. 11th SOFT, Oxford 1980, p. 387.
[40] U. Broßmann, Proc. 11th SOFT, Oxford 1980, p. 473.
[41] W. D. Haubenberger, Proc. 11th SOFT, Oxford 1980, p. 479.
[42] W. D. Haubenberger, Proc. 9th Symposium on Engineering Problems of Fusion Research, Chicago 1981, p. 189.
[43] Technical Specification of a Tokamak Poloidal Field Coil System with special consideration of the central coil with a magnetic field of extremely high value, E. Harmeyer, M. Kollotzek, M. Pillsticker, W. Wanner, and F. Werner, IPP Garching Report 1/196 November 1981.
[44] Stressing of the ZEPHYR Vacuum Vessel by Plasma Disruptions, H. Kotzlowski, F. Mast, and H. Preis, IPP Garching Report 1/175 (1981).
[45] H. Kotzlowski, Proc. 9th Symposium on Engineering Problems of Fusion Research, Chicago 1981, p. 1626.
[46] H. Krause, H. Brockmann, and U. Ohlig, Proc. 11th SOFT, Oxford 1980, p. 247.
[47] G. Prillinger, A. Fischer, E. Fischer, and H. Krause, Nuclear Technology/Fusion **2**, 301 (1982).
[48] ZEPHYR Tritium System, C. Andelfinger, E. Buchelt, J. Fink, and H. Weichselgartner, IPP Garching Report 1/203 (1982).
[49] J. Perchermeier and H. Weichselgartner, Proc. 11th SOFT, Oxford 1980, p. 571.